

# Kiso H $\alpha$ Imaging Observations of Nearby Galaxies

T. Hasegawa<sup>1</sup>, S. Sakamoto<sup>2</sup>, S. Nishiura<sup>3</sup>,  
Y. Ohyama<sup>3</sup> and Y. Sofue<sup>1</sup>

<sup>1</sup> Kiso Observatory, University of Tokyo, 10762–30, Mitake, Kiso, Nagano 397–01, Japan  
htakashi@mtk.ioa.s.u-tokyo.ac.jp

<sup>2</sup> Nobeyama Radio Observatory, National Astronomical Observatory of Japan,  
Minamimaki, Minamisaku, Nagano 384–13, Japan  
seiichi@nro.nao.ac.jp

<sup>3</sup> Department of Astronomy, Tohoku University,  
Aoba, Sendai, Miyagi 980–77, Japan

**Abstract:** We report H $\alpha$  imaging observations of nearby galaxies with the Kiso Schmidt telescope. For spiral galaxy NGC 628, we found no clear correlation between H $\alpha$  and CO intensities, and we discuss the star formation efficiency of this galaxy. No nuclear H $\alpha$  emission in this galaxy was detected. This is consistent with spectroscopic observations which indicate that the nuclear region is in the post starburst phase. We also describe the H $\alpha$  image of Hickson’s compact group 92 in which diffuse emission is detected extending within the group system.

**Keywords:** galaxies: ISM — infrared: galaxies — radio lines: galaxies.

## 1 Introduction

For narrow-band H $\alpha$  imaging observations of nearby galaxies, we have two advantages in using the 105 cm Schmidt telescope at the Kiso Observatory. First, the small  $f/3.1$  focal ratio of this telescope yields efficient detection of extended diffuse light. Second, an installed CCD camera with 1024 square pixels (TI215) has a field of view of  $12.5 \times 12.5$  arcminutes which is wide enough to cover nearby galaxies with large angular size.

The goal of our narrow-band imaging observations is to investigate the factors which regulate the star formation efficiency (SFE). The SFE can be estimated as the fraction of the mass of on-going star formation measured from the H $\alpha$  intensity over the molecular gas mass from the CO intensity. A number of nearby galaxies have been observed with CO emission at the Nobeyama Radio Observatory (NRO). However, very small numbers of such galaxies have been observed at H $\alpha$ . Hence we have begun to obtain a homogeneous set of H $\alpha$  images of these galaxies with the Kiso Schmidt telescope. Along with K’-band images, we investigate the effect on the SFE from factors such as gas density, galactic structures (arms and bars), morphology, and environment. The star formation *rate* has been studied case by case in the context of threshold gas surface density (Kennicutt 1989; Kuno et al. 1995; Hunter & Plummer 1996). We study not only the star formation *efficiency* (H $\alpha$ /CO) but also the star formation *rate* (H $\alpha$ ), based on the forthcoming homogeneous set of H $\alpha$  images.

We have selected more than 30 isolated face-on spiral and dwarf galaxies and have so far observed 10 of them, including NGC 628 (M74), NGC 6946, NGC 5236 (M83) and IC 10. We also observed Hickson’s (1994) compact group HCG92 to assess environmental effects.

## 2 Star Formation Efficiency of NGC 628

An isolated face-on spiral galaxy NGC 628 was observed with two narrow-band ( $\Delta\lambda = 20 \text{ \AA}$ ) interference filters centred on and off the H $\alpha$  line. The seeing size was 3.5 arcsec. Standard bias-subtraction, flat-fielding and sky-subtraction was applied. We subtracted continuum light by scaling the flux of about 10 Galactic stars to obtain the H $\alpha$  image (Figure 1), which is very similar to the image obtained by Belley & Roy (1992).

The CO ( $J = 1-0$ ) map of the central 4 arcmin square region (Figure 1, right) was obtained with the NRO 45 m telescope (HPBW = 14 arcsec). The grid was taken along the major and minor axes of the galaxy with 11 arcsec spacing.

The K’-band image was obtained with an infrared camera OASIS attached to the 188 cm reflector at the Okayama Astronomical Observatory (OAO). The seeing was 2 arcsec. We subtracted a rotationally averaged component to extract arms and any possible embedded bar component. The resultant image, which we refer to as the *dK* image, is shown in the left panel of Figure 1. We obtained spectra for the nuclear region and an HII region at OAO (Figure 2).

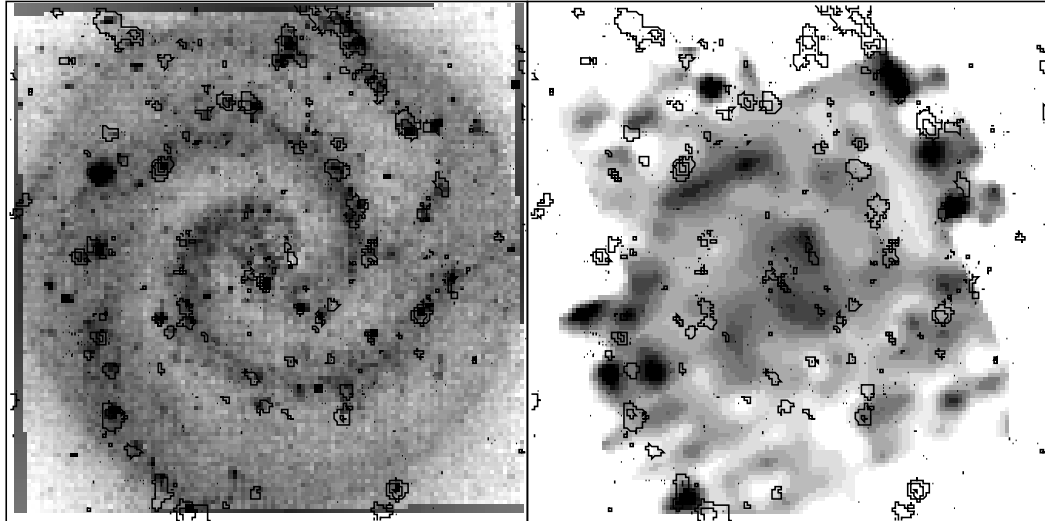


**Figure 1**—The  $dK$  image (see text, *left panel*) and CO ( $J = 1-0$ ) map (*right panel*) of NGC 628 with linear scale intensity. Contours indicate logarithmic  $H\alpha$  intensity with an interval of 0.6. The central 4 arcmin (which corresponds to 8 kpc) is shown. North is top and east is to the left.

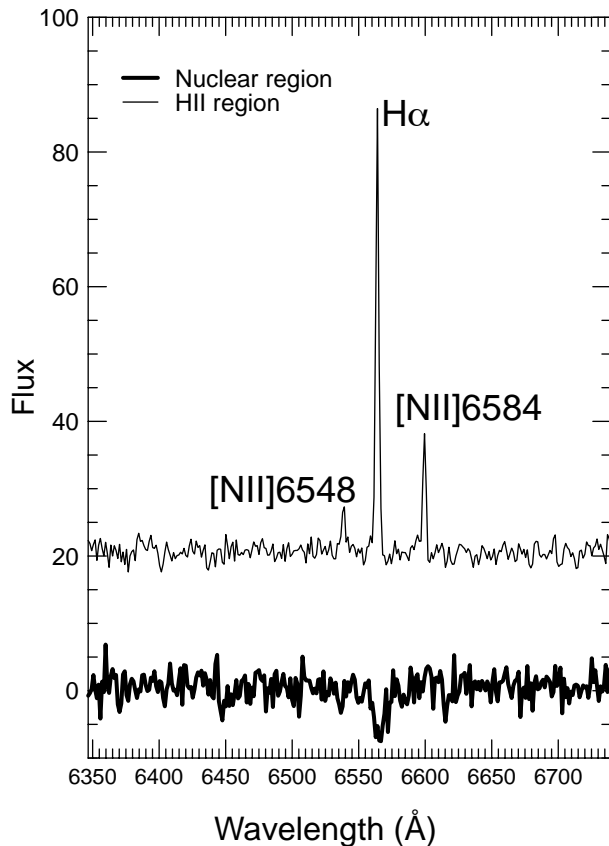


**Figure 2**—Spectra of NGC 628 at its nuclear region (*thick line*) and at an HII region (*thin line*). The spectrum at the HII region is shifted vertically for clarity.

In the  $dK$  image, two spiral arms are clearly identified while no bar is discernible. Regions with strong  $H\alpha$  and CO emission are predominantly located along these spiral arms. Most of the bright spots in the  $dK$  image are identified with  $H\alpha$  emission (Figure 1).

If the SFE is uniform over the entire galaxy, a tight correlation is expected between  $H\alpha$  and CO intensities. Unexpectedly, the peaks of  $H\alpha$  and CO emission are poorly correlated within 1 kpc. We find many giant HII regions in the outer part of the arms, but even these regions are hardly identified with giant molecular clouds. We find no giant HII regions at two giant molecular clouds located close to the centre. The extinction in the HII region of this galaxy is small (Belley & Roy 1992). The poor correlation between identified  $H\alpha$  and CO peaks may suggest that the SFE is not uniform in this galaxy and is regulated not only by the mass of molecular clouds but also by other physical parameters, such as the velocity dispersion of the molecular clouds. Alternatively,  $H\alpha$  and CO emission may represent two different evolutionary stages of star formation. The poor correlation observed is contrary to the case of M51, in which most of the giant HII regions are identified with giant molecular clouds (Kuno et al. 1995).

We detect no nuclear  $H\alpha$  emission. A slight overestimate (3–5%) of the scaling factor in the subtraction of continuum light might lead to an underestimate of the nuclear  $H\alpha$  emission by a about 20%. However, the spectrum at the nuclear region (Figure 2, thick line) indicates that  $H\alpha$  is actually seen in absorption here. Since the absorption at  $H\alpha$  is typical for spectra of late-B and A-type stars (Gunn & Stryker 1983), the absorption at the nuclear region of the galaxy suggests that these stars are the high-mass end of the present-day mass function and the nuclear region is in the post-starburst phase.

### 3 Star Formation in HCG 92

We briefly describe  $H\alpha$  and archival B-band images (by Mendes de Oliveira) of HCG 92, which is

composed of three interacting galaxies. Diffuse  $H\alpha$  emission is detected at  $5\sigma$  above the noise level, extending as far as the system of HCG 92 itself. This diffuse emission suggests that the three galaxies in HCG 92 are interacting with each other. One galaxy is of Seyfert type II, and it is consistent with the intense nuclear emission in the  $H\alpha$  image. Giant HII regions are identified on tidal tails of two remaining galaxies. However, nuclear star formation of these galaxies is neither confirmed from the  $H\alpha$  image nor from the spectroscopy.

- Belley, J., & Roy, J. R. 1992, *ApJS*, 78, 61  
Gunn, J. E., & Stryker, L. L. 1983, *ApJS*, 52, 121  
Hickson, P. 1994, *Atlas of Compact Groups of Galaxies*  
(New York: Gordon & Breach)  
Hunter, D., & Plummer, J. D. 1996, *ApJ*, 462, 732  
Kennicutt, R. C. 1989, *ApJ*, 344, 685  
Kuno, N., et al. 1995, *PASJ*, 47, 745  
Sofue, Y. 1993, *PASP*, 105, 308